RD_Mucol/LNF 2025

C. Cantone, A. Cemmi (Associata), V. L. Ciccarella (Dottoranda), F. Colao (Associato),
E. Di Meco (Dottoranda), I. Di Sarcina (Associata), R. Gargiulo (Dottorando),
F. Happacher, I. Sarra (Responsabile Locale),
J. Scifo (Associata), R. Soleti (Associato), A. Verna (Associato)

in collaboration with:
"LNF-SEA": S. Ceravolo (Tecnico)
"Servizio Progettazione e Costruzioni Meccaniche": T. Napolitano
the Detectors Development and Construction Unit: A. Russo (Tecnico)
and the BTF team member E. Diociaiuti (Art. 36).

The Muon Collider [1] is being proposed as a future high-energy physics facility exploiting the unique properties of muons for multi-TeV collisions. Owing to their larger mass, muons emit significantly less synchrotron radiation than electrons; however, their decay products generate intense Beam-Induced Backgrounds (BIB), which pose major challenges for detector systems. In the electromagnetic calorimeter (ECAL) region, simulations predict fluxes of approximately 300 particles per cm^2, dominated by photons (96%) and neutrons (4%), with an average photon energy of about 1.7 MeV. Detectors must cope with these high level of background. Radiation levels have been quantified through FLUKA simulations at $\sqrt{s} = 1.5$ TeV: in the ECAL barrel region, the expected neutron fluence reaches 10^{14} n_{1MeV}/cm^2 per year, with a corresponding Total Ionizing Dose (TID) of approximately 1 kGy per year.

A W-Si sampling calorimeter inspired by the CALICE design was initially considered as a reference solution. While offering good performance, this approach involves substantial system complexity and cost. The Crilin calorimeter [2] has been developed as a more compact and cost-effective solution designed to operate in the high-background and high-radiation environment of the Muon Collider.

1 The Crilin Calorimeter

The Crilin calorimeter is being developed as a candidate electromagnetic calorimeter for a future Muon Collider, designed to operate in a high-background and high-radiation environment. The detector is based on a semi-homogeneous architecture using high-density crystal matrices, with each unit equipped with two independent readout channels. This configuration combines fast timing, fine spatial granularity, longitudinal segmentation and radiation hardness within a compact and scalable system.

1.1 Detector Architecture

The mechanical and geometrical design of the Crilin calorimeter is driven by the requirement of sub-100 ps timing, essential for effective BIB rejection, while preserving compactness and system simplicity. The detector is based on modular crystal matrices, where each crystal is independently read out by two channels, each integrating a pair of Silicon Photo-Multipliers (SiPMs). This architecture provides fine spatial resolution, defined by a cell size of 10×10 mm^2, granting an efficient separation of background from physics signals and limiting pile-up.

The overall geometry is optimized to reduce channel occupancy, improve hit separation, and support efficient clustering and reconstruction in high-rate conditions. Longitudinal segmentation is implemented through the layered structure, with each detection layer having a total thickness

of 45 mm, comprising 40 mm of crystal and 5 mm for the readout system. This compact layout is central for the identification and suppression of BIB-induced energy deposits.

Compared to conventional W-Si sampling calorimeters, the Crilin design requires a reduced number of layers and readout channels, simplifying electronics integration and reducing overall system complexity and cost, without compromising performance.

1.1.1 Material Selection and Radiation Hardness

The Crilin calorimeter employs radiation-resistant crystal materials, in particular PbF_2 [4] and $PbWO_4$-UF [5], which have demonstrated stable performance under high radiation exposure. PbF_2 crystals preserve their optical transmittance after irradiation up to 260 kGy TID, as tested at the Calliope gamma facility (ENEA NUC-IRAD-GAM Laboratory). $PbWO_4$-UF crystals withstand doses up to 1.5 MGy [3].

Radiation tolerance has been extensively evaluated for the photosensors as well. Hamamatsu S14160-3010PS SiPMs, featuring a 10 µm pixel size, exhibit only a limited increase in dark current after irradiation to a neutron fluence of 10^{14} $n_{1MeV\text{-}eq}/cm^2$ and a TID of 10 kGy. Their performance is superior to that of the S14160-3015PS devices with 15 µm pixels, supporting their selection for operation in high-radiation environments.

These qualification results are consistent with the expected radiation levels at the Muon Collider, of the order of 1 kGy/year TID and neutron fluences up to 10^{14} $n_{1MeV\text{-}eq}/cm^2$, and confirm the suitability of the chosen materials and sensors for long-term, reliable calorimeter operation.

1.1.2 Performance Evaluation

The Crilin ECAL has been studied through detailed simulations and experimental tests, showing consistent performance. Simulations in the Muon Collider framework yield an energy resolution of $\sigma_E/E \approx 4.8\%/\sqrt{E} \oplus 0.2\%$ for photons, which is competitive with conventional sampling calorimeters. In the presence of Beam-Induced Backgrounds, the resolution degrades as expected, reaching $10.7\%/\sqrt{E} \oplus 0.95\%$ and remaining compatible with the Muon Collider requirements. Ongoing developments in clustering and reconstruction algorithms aim to better exploit longitudinal information and further suppress BIB-induced fluctuations. The corresponding results are shown in Figure 1.

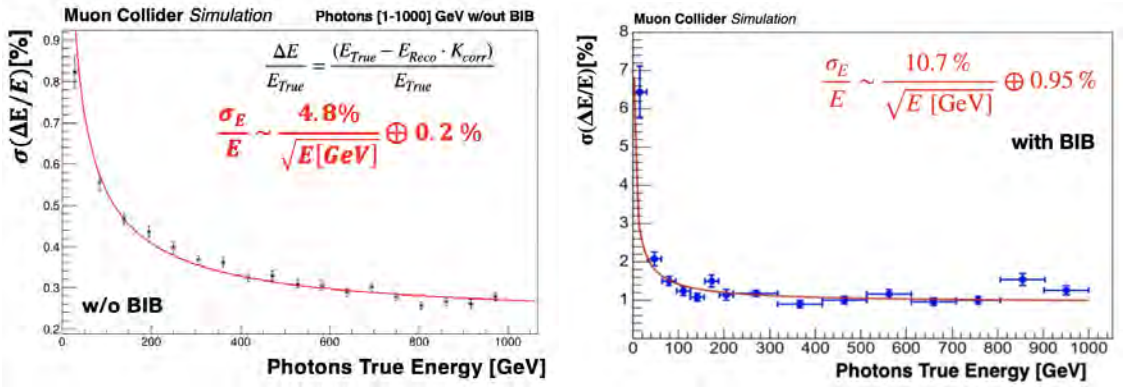

Figure 1: Simulated energy resolution in the Muon Collider framework without (left) and with (right) BIB contributions.

During the first stages of the R&D, two prototype detectors have been developed and tested. Proto-0 [6], composed of two crystals and four readout channels, and Proto-1, consisting of two

layers of a 3×3 crystal matrix read out by 36 channels, both demonstrated excellent timing performance, at the level of $\mathcal{O}(20$ ps), and good agreement with Monte Carlo simulations, validating the detector concept.

In August 2023, the timing performance of Proto-1 was measured with a 120 GeV electron beam at the CERN-SPS H2 beamline. The analysis focused on the central crystals of the matrix, where the highest energy deposits occur. As shown in Figure 2-left, the prototype achieved a single-crystal time resolution below 40 ps for energy deposits above 1 GeV. The inter-layer timing performance was evaluated using the time difference between the two most energetic crystals in different layers. The distribution, shown in Figure 2-right, was fitted with a Double Sided Crystal Ball function, yielding a resolution of $\sigma_{\Delta t} = 45$ ps. This value is dominated by digitizer synchronization jitter, measured to be $\mathcal{O}(32$ ps) for board-to-board and $\mathcal{O}(10$ ps) for channel-to-channel configurations.

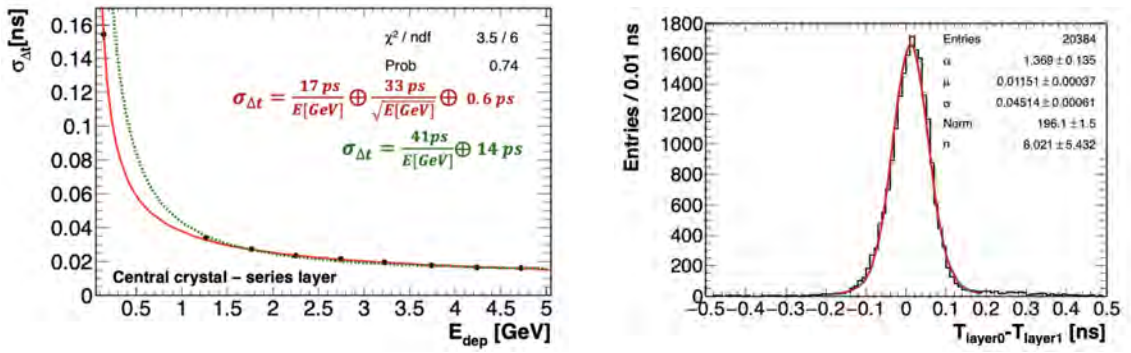

Figure 2: Left: time resolution as a function of the energy deposited in the crystal with the highest energy deposit; an additional 450 MeV electron beam data point is shown by the red fit. Right: time resolution of the time difference between the two most energetic crystals in different layers.

1.2 Prototype Development

During 2025, Crilin R&D activities focused on the construction and operation of a new prototype, Proto-2, aimed at validating the final detector concept both in terms of mechanics and electronics upgrades.

1.2.1 Proto-2

Proto-2 consists of a single-layer 3×3 crystal matrix, read out by 9 channels, each composed by 2 $3{\times}3$ mm^2 SiPMs. The new mechanical structure is based on an innovative aluminum alveolar matrix, visible in Figures left and central panel, with 150 µm inter-crystal septa, providing high mechanical stability while reducing inactive material. The readout system was upgraded with faster, custom-designed front-end electronics boards (Figure 3-right), to improve timing performance and signal shaping with respect to previous prototypes.

1.2.2 Beam hodoscope

A dedicated beam hodoscope, shown in Figure 4-left, was developed to support beam test activities by providing precise beam profiling and event-by-event tracking. This system allows spatially resolved studies of the calorimeter response as a function of the particle impact position.

Figure 3: Proto-2, equipped with LYSO crystals for a cosmic ray test prior to beam operations (left, center) and front-end electronics board (right).

The hodoscope is a biplanar detector based on plastic scintillating tiles read out by 4×4 SiPM arrays in a light-sharing configuration (visible in Figure 4-right), providing fine spatial resolution within a compact layout. Signal amplification, shaping and digitization are provided by the same FEE and CAEN V1742 switch capacitors used for Crilin. The detector is housed in a custom 3D-printed mechanical structure designed to ensure stable positioning and fit on a 2 stage motorized structure, allowing remote adjustment and precise alignment with the beam.

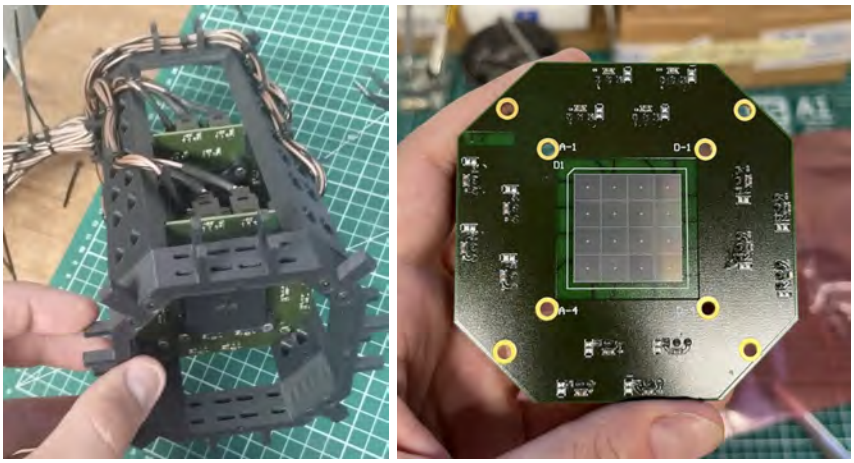

Figure 4: Beam hodoscope, with the two detector planes embedded in the mechanical structure (left), and SiPM board (right).

1.3 2025 beam test campaigns

1.3.1 Beam test at CERN SPS

In September 2025 a beam test campaign was carried out at CERN SPS using electron beams of energies of 60, 100 and 140 GeV. The campaign aimed at the characterization of Proto-2's front-end electronics and DAQ system, based on 2 CAEN V1742 digitizer boards. Figure 5 (top) shows the experimental setup with the main components highlighted, while Figure 5 (bottom) presents the detector layout. Passive PbF_2 crystal matrices were also added to the setup to emulate the

response of second and third calorimeter layers, useful for multi-layer studies.

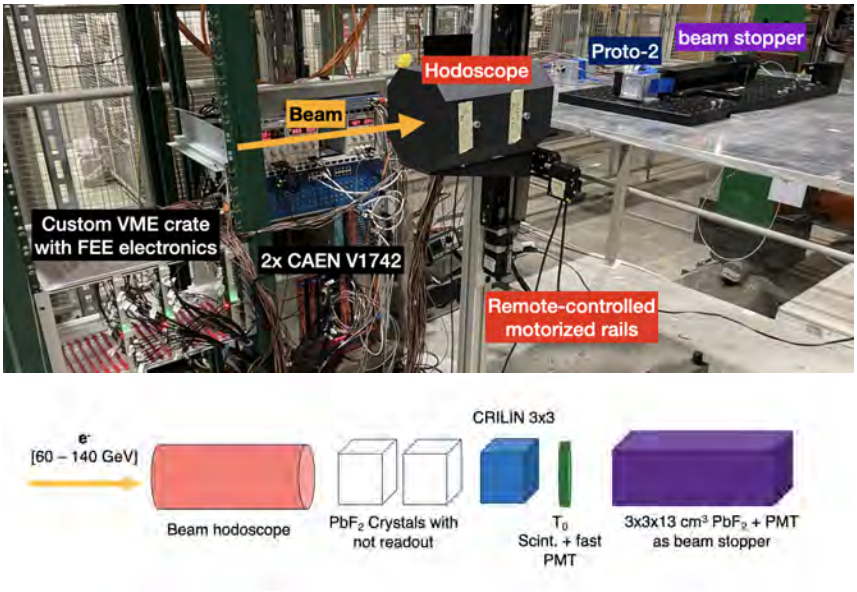

Figure 5: Top: picture of the September 2025 beam test setup at CERN SPS, with main components highlighted. Bottom: scheme of the beam test detector layout.

One of the aims of the campaign was to finalize the single-layer electronics gain for the upcoming full-scale prototype by comparing simulated and measured energy deposition profiles across the detector layers. Figure 6-left shows the energy deposited per layer for electron beams of 60, 100, and 140 GeV, demonstrating good agreement between experimental data and simulations. This validates both the detector modeling and the reconstruction chain. This test allowed to select a suitable electronics gain for each layer, in order to maximize the signal to noise ratio at layer level.

The performance of the beam hodoscope was evaluated in terms of spatial resolution. Figure 6-right shows a resolution of ∼200 µm along the horizontal axis, with comparable performance along the vertical direction, confirming the ability to provide a reliable event-by-event tracking.

1.3.2 Beam test at LNF BTF

In December 2025, a beam test campaign was carried out at the Frascati Beam Test Facility (BTF) using a 500 MeV electron beam with sub-millimeter spot size. The beam was delivered in 10 ns bunches, with a particle multiplicity of 30 per bunch. The FEE electronics gain were significantly increased (from 0.5 up to 8) to allow the detection of particles at this energy.

The measurements focused on the characterization of different reflective crystal wrapping configurations and their impact on the prototype response in terms of collected charge. Figure 7 shows the single-channel charge distributions measured for four different wrapping materials (Teflon, Mylar, vinyl, and aluminum). The distributions were fitted with Gaussian functions to extract the mean charge values and their spreads. While the charge resolution is comparable for all configurations, clear differences are observed in the collected charge mean value. The highest light output, corresponding to the largest deposited charge, is obtained with the wrapping composed of three layers of Teflon and two layers of aluminum coating, wrapping that will be used in the upcoming full-scale prototype.

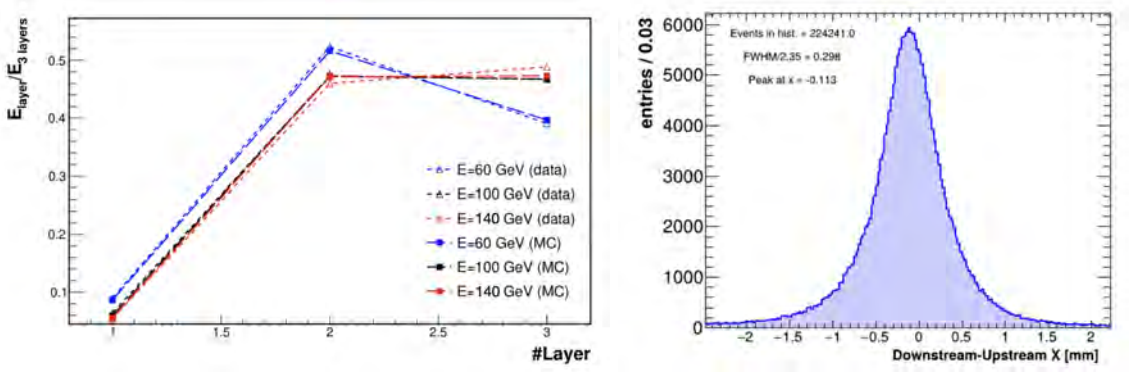

Figure 6: Results from the September 2025 beam test campaign. Left: comparison of simulated and experimental energy deposition per layer, for electron beam energies of 60, 100 and 140 GeV. Right: beam hodoscope energy resolution along the horizontal axis. The resolution along the vertical axis is comparable.

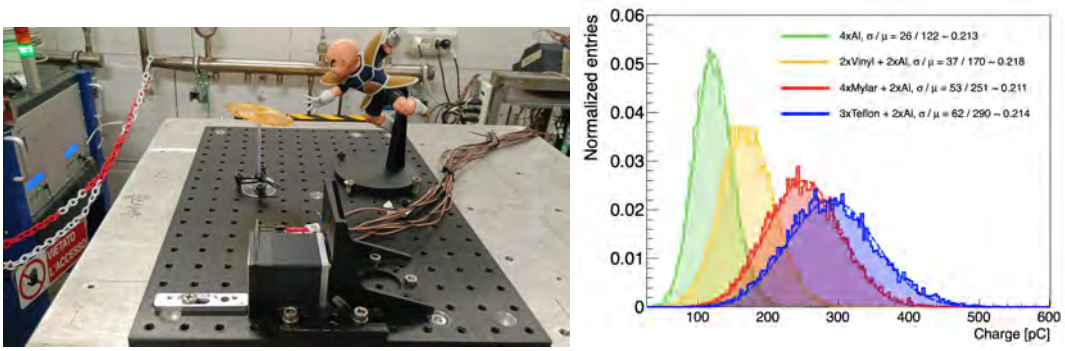

Figure 7: Left: picture of the December 2025 beam test setup at the Frascati BTF. Right: Proto-2 single-channel charge distribution for four different crystal wrapping configurations.

1.4 Full-scale Prototype

As mentioned above a new full-scale prototype of the Crilin technology has been thoroughly designed during 2025 and will be fully assembled and tested throughout 2026. The detector will consist of five layers of 7×7 PbF_2 crystal matrices, covering approximately 2 Molière radii (R_M) and 26 radiation lengths (X_0). The selected crystals have a cross section of 1.3×1.3 cm^2, with a tolerance of 0.1 mm.

The mechanical and electronic design integrates the solutions validated with Proto-2. The crystal matrices will be housed in an aluminum alveolar structure with 150 µm inter-crystal septa, while a 2 mm thick external envelope will surround the matrix; a first production of the aluminum matrix (1 layer) was already finalized in 2025 as can be seen in Figure 8-left. A micro-coaxial Kapton strip will provide SiPM polarization and readout independently for each channel of two SiPMs in series. An overall connector will be placed at the back of the five assembled modules. A 3D model of the final Crilin prototype is shown in Figure 8-right.

This final configuration provides enough containment to allow dedicated studies of energy resolution together with the timing performance. The expected energy resolution was evaluated with a Monte Carlo simulation, inserting Light Yield and Gaussian noise estimates from beam

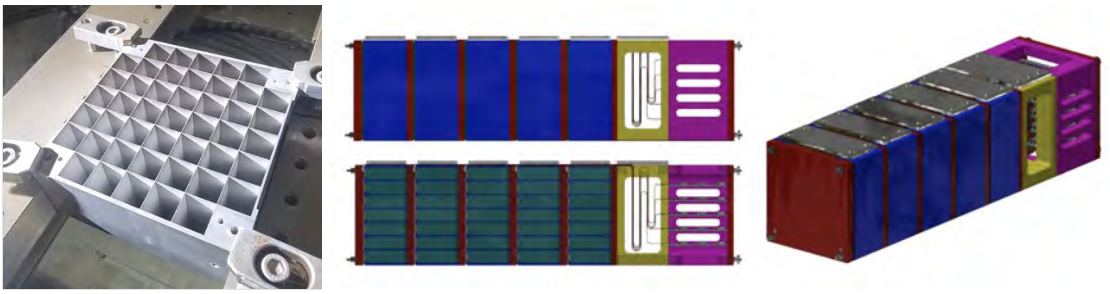

Figure 8: Left: Production of the first 7×7 aluminum alveolar structure. Right: 3D model of the final prototype mechanics embedding five layers of 7×7 crystal matrices.

tests, and a 30 MeV energy threshold on single crystals. The results, reported in Figure 9, show promising results with a stochastic term of approximately 7.6%.

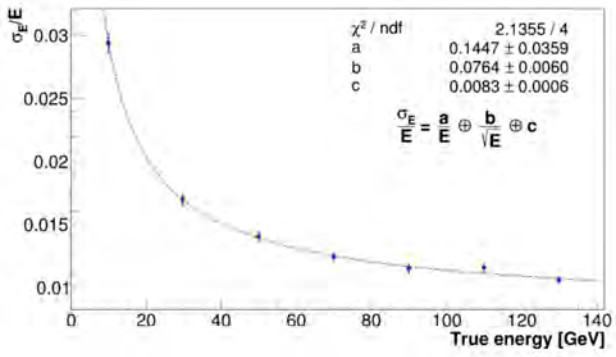

Figure 9: Simulated energy resolution of the final prototype.

2 List of Conference Talks/Posters by LNF Authors in the Year 2025

1. E. Di Meco, The CRILIN technology: an optimised calorimeter solution for a future Muon Collider, INFN Workshop for Future Detectors 2025, Sestri Levante, IT.
2. E. Di Meco, Optimising an ECAL barrel for a Muon Collider: the Crilin design, Muon4Future 2025, Venice, IT.
3. E. Di Meco, Crilin: a highly granular semi-homogeneous crystal calorimeter with excellent timing for future colliders, EPS 2025, Marseille, FR.
4. I. Sarra, Development and Test of the CRILIN Calorimeter for the Muon Collider: Status and Perspectives, 2025 IEEE NSS MIC RTSD, Yokohama, JP.

3 Publications

- C. Cantone, et al., "Advancements in Muon Collider Calorimetry: Design, Testing, and Radiation Resistance of the Crilin Calorimeter Prototype", EPJ Web Conf. 320 (2025) 00023. DOI: https://doi.org/10.1051/epjconf/202532000023.

- C. Cantone, et al., "CRILIN: A semi-homogeneous crystal calorimeter for the Muon Collider", Nuovo Cim.C 48 (2025) 3, 112. DOI: https://doi.org/10.1393/ncc/i2025-25112-4.
- C. Cantone, et al., "Crilin: A novel calorimeter proposal for the $\sqrt{s}$= 10 TeV Muon Collider — Simulations and prototype tests results", Nucl.Instrum.Meth.A 1079 (2025) 170617. DOI: https://doi.org/10.1016/j.nima.2025.170617.
- A. Cemmi, et al., "Radiation Resistance of the Muon Collider CRILIN Calorimeter Prototype Equipped With Cherenkov Lead Fluoride Crystals", IEEE Trans.Nucl.Sci. 72 (2025) 7, 2012-2020. DOI: https://doi.org/10.1109/TNS.2025.3544810.
- I. Sarra, "Development and Test of the CRILIN Calorimeter for the Muon Collider: Status and Perspectives", Contribution to: 2025 IEEE NSS MIC RTSD.
  DOI: https://doi.org/10.1109/NSS/MIC/RTSD57106.2025.11287199.
- P. Andreetto, et al., "MUSIC: A Multi-Purpose Detector Concept for Physics at the 10 TeV Muon Collider". DOI: https://doi.org/10.48550/arXiv.2511.23273.

References

1. C. Accettura et al., *Towards a Muon Collider*, Eur. Phys. J. C (2023) 83: 864; DOI: `https://doi.org/10.1140/epjc/s10052-023-11889-x`.
2. S. Ceravolo et al., *Crilin: A CRystal calorImeter with Longitudinal InformatioN for a future Muon Collider*, JINST 17 P09033 (2022); DOI: `10.1088/1748-0221/17/09/P09033`.
3. C. Cantone et al., *R&D status for an innovative crystal calorimeter for the future Muon Collider*, IEEE Transactions on Nuclear Science PP(99):1-1 (2024); DOI: `10.1109/TNS.2024.3364771`.
4. A. Cemmi et al., *The CRILIN calorimeter: gamma radiation resistance of crystals and SiPMs*, JINST 19 P10016 (2024); DOI: `10.1088/1748-0221/19/10/P10016`.
5. M. Korzhik. et al., *Ultrafast PWO scintillator for future high energy physics instrumentation*, Nucl. Instrum. Meth. A 1034 (2022); DOI: `10.1016/j.nima.2022.166781`.
6. C. Cantone et al., *Beam test, simulation, and performance evaluation of PbF2 and PWO-UF crystals with SiPM readout for a semi-homogeneous calorimeter prototype with longitudinal segmentation*, Frontiers in Physics 11 (2023); DOI: `10.3389/fphy.2023.1223183`.